

Fifth-Power Altitude Dependence of Particle Precipitation at The Minimum Geomagnetic Field Position

M. M. Adel¹

Department of Chemistry & Physics, University of Arkansas at Pine Bluff, Pine Bluff, AR 71601, USA

Abstract: The fifth power altitude dependence of magnetospheric particle precipitation near the geomagnetic equator in the altitude range of 160 to 300 km during moderate geomagnetic conditions has been explained. In the atmosphere, the observed altitude dependence of proton flux can be due to a number of factors such as (i) source attenuation, (ii) charge exchange loss of protons, (iii) proton loss due to atmospheric ionization, and (iv) proton loss due to pitch angle diffusion in the loss cone. Each of these causes has been discussed to estimate the importance in the explanation of the observed proton flux variation with altitude

I. INTRODUCTION

Magnetospheric particle precipitation in the atmosphere has been studied since the seventies of the last century using particle telescopes on board satellites (Hovestadt et al., 1972; Moritz, 1972; Mizera and Blake, 1973; Scholer et al., 1975). A number of articles have reported the observation of the global peak flux profile, energy spectra, solar cycle variation and the instrument efficiency function for detection particles of different pitch angles by the ONR-602 experiment on board the S81-1 pallet mission (Miah et al., 1988; Miah et al., 1989; Miah, 1989; 1990; Miah, 1991a; Miah, 1991b; Miah, 1993; Miah, 1993b; Miah, 1994a; Miah, 1994b; Adel, 2008; Adel, 2012; Adel, 2013). In the altitude range of 160 km to about 300 km of observation during moderate geomagnetic conditions the flux of proton precipitation near the minimum geomagnetic field exhibit a variation of the fifth power of altitude (Fig. 1). In the atmosphere, the observed altitude dependence of proton flux can be due to several factors which are (i) source attenuation, (ii) charge exchange loss of protons, (iii) proton loss due to atmospheric ionization, and (iv) proton loss due to pitch angle diffusion in the loss cone. This article explores all these possible reasons that have contributed to the altitude variation.

II. MATERIALS AND METHOD

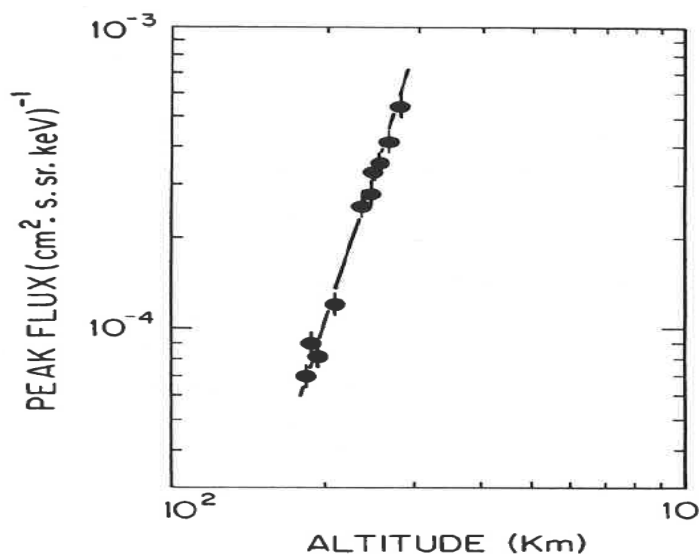


Fig 1. The fifth-power altitude dependence of the flux of protons precipitated from the magnetosphere at low equatorial altitude

¹ Corresponding Author: adelm@uapb.edu

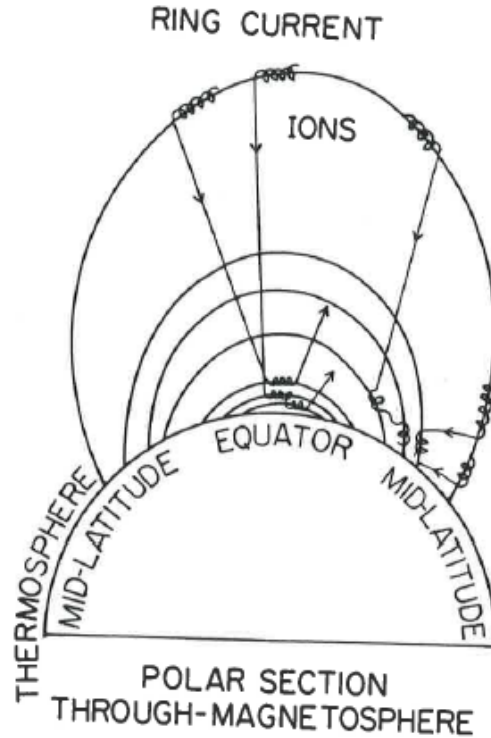


Fig2. Illustration of charge-exchange reaction

2.1. Coulomb Interactions

Another loss effect is though energy loss due to Coulomb interactions. But this is, comparatively, a much weaker process, as can be understood in these two examples: At 150 km a proton with an equatorial pitch angle of $\alpha_e=90^\circ$ and $E=1$ MeV, has an electron capture lifetime of 0.4sec. and during this lifetime it loses ~ 162 keV and still remains as a proton for a long time. At 300 km which is the other extreme end (relative to the observational altitude range of 165-285 km), the same proton loses 2.64 keV in its charge exchange lifetime of 34.3 secs. So, the energy loss process can be neglected unless some threshold energy value is specified below which the proton will be considered lost.

2.2. Pitch Angle Diffusion

The third loss effect is pitch angle diffusion. A proton during its charge exchange lifetime undergoes some scattering in pitch angle. If the pitch angle increases in the multiple Coulomb scattering process, the proton stays quasitrapped. If the pitch angle decreases, the proton has to mirror at a higher latitude λ_M i.e. lower atmosphere and be lost into the atmosphere. The relationship between the mirror latitude and the equatorial pitch angle is

$$\sin^2 \alpha_e = \text{Cos}^6 \lambda_M / (1 + 3 \sin^2 \lambda_M)^{0.5} \quad (1)$$

$$\text{or, approximately } \sin \alpha_e = \text{cos}^4 \lambda_M \quad (2)$$

Also, the loss cone size is an equatorial altitude dependent function. Usually, the loss cone size α_o is defined with respect to the mirror point at 100 km which is taken as the effective edge of the atmosphere i. e.

$$\alpha_o(r_o) = \sin^{-1} [B_e(r_o)/B_{100}]^{0.5} \quad (3)$$

All particle with α_e between 0 and α_o mirror at ≤ 100 km and are dumped into the atmosphere.

As shown in Table I below, the dipole field can trap particles of certain equatorial pitch angle range. L is the geocentric equatorial distance of a field line in units of the Earth's radius. The appropriate loss factor in this case is the ratio of the integral of the pitch angle distribution function within the pitch angle range at the altitude under consideration to the same integral between the pitch angle range at the normalization altitude (say 800 km). Because the pitch angle distribution function is sharply peaked at $\alpha_e=90^\circ$, this ratio is weakly dependent upon altitude. For

the time being the inclusion of this ratio in the equation for the equilibrium situation is omitted. The ratio is important in combination with the instrument's sampling efficiency in pitch angle space.

Table1. Dipole Field-Trappable Particle with Equatorial Pitch Angles

L	Equatorial Altitude (km)	Equatorial Pitch Angle (deg.)
1.02354	150.00	~ 80 – 1000
1.03139	200.00	~ 76 - 104
1.03924	250.00	~ 73 - 107
1.04708	300.00	~ 70 - 110
1.05493	350.00	~ 68 – 112
1.06278	400.00	~ 66 – 114
1.07063	450.00	~ 64 – 116
1.07848	500.00	~ 62 – 118
1.08633	550.00	~ 61 – 119
1.09418	600.00	~ 59 – 121
1.10202	650.00	~ 58 – 122
1.10987	700.00	~ 57 – 123
1.11772	750.00	~ 56 – 126
1.12557	800.00	~ 54 – 126
1.13342	850.00	~ 53 – 127
1.14126	900.00	~ 51 – 129
1.14911	950.00	~ 50 – 130
1. 15696	1000.00	~ 49 – 131

At any time t and at any altitude h the equation describing generation and loss of protons of $\alpha_e=90^\circ$ can be written as Accumulation rate of proton flux = generation rate of proton flux – loss rate of proton flux , i.e.

$$\frac{dj_p(E, h)}{dt} = v [\sum_{01} (h, E)] j_H (E, h) - v[\sum_{10} (h, E)] j_p (E, h) \quad (4)$$

where $j_p(E, h)$ is the differential proton flux ($\text{cm}^2\text{-s-sr-keV}^{-1}$);

$j_H(E, h)$ is the differential neutral hydrogen flux ($\text{cm}^2\text{-s-sr-keV}^{-1}$);

$$\sum_{01} (h, E) = \sum n(E, h)_i (\sigma_{01} (E)) \quad (\text{cm}^{-1}) \quad (5)$$

is the sum of the products of the atmospheric constituents and their electron stripping cross-sections for energetic neutral hydrogen

$$\sum_{10} (h, E) = \sum \check{n}(E, h)_i (\sigma_{10} (E))_i \quad (\text{cm}^{-1}) \quad (6)$$

is the sum of the products of bounce average density of atmospheric constituents (Fig. 3) and the electron capture cross sections for protons (Toburen et al., 1968); and v is the velocity of the energetic neutrals or of the energetic protons.

The lifetime against neutralization is defined as

$$\tau_{CE}(h, \alpha_e) = [\sum \check{n}(E, h)_i (\sigma_{10} (E))_i v]^{-1} \quad (7)$$

is a strong function of proton energy and a weak function of pitch angle.

For an equilibrium condition, Eq. (4) yields

$$\frac{J_H(E, h) \sum_{01}(h, E)}{\sum_{10}(h, E)} = j_p(E, h) \quad (8)$$

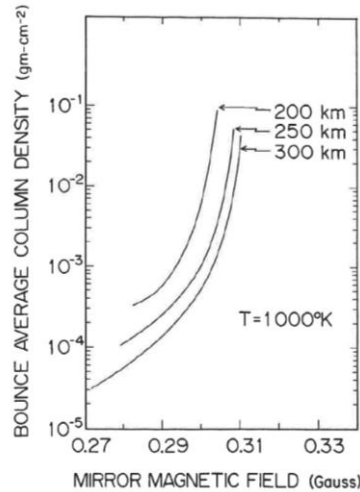


Fig3. Bounce average atmospheric column density vs mirror point magnetic fields for three different equatorial altitudes.

Fig. 4 illustrates the mechanism of charged particle trapping in the geomagnetic field. For equatorially mirroring particles of $\alpha_e=90^\circ$, n_i is the same as \bar{n}_i (cyclotron orbit average density was not calculated since cyclotron radius \ll density scale height), so, for these particles the ratio in Eq. (8) is effectively a function of energy through the ratios of electron capture to electron loss cross sections. Eq. (8) shows that any dependence of j_p on altitude can be introduced through the altitude dependence of j_H .

To investigate the depletion of source neutrals as a function of both energy and altitude, the fraction of the surviving neutrals at any altitude was calculated. This fraction is given by

$$W_{AT}(E, h) = e^{-\sum S(h)_i \sigma_{0i}(E)_i} \quad (9)$$

where $S(h)_i$ is the column density of the i th atmospheric constituent, and the sum runs over all the atmospheric constituents. In a spherically symmetric atmosphere, at a given altitude in the equatorial plane, column densities (starting from 2500 km) of individual gases in the zenith angle range $-90^\circ \leq \theta \leq 90^\circ$ (which takes care $\sim 30\%$ of the equatorial part of the L shells in the range 2.5 – 3.5) was calculated at intervals of 1° . The column densities were multiplied by the electron stripping cross sections of the individual gases, and the fraction in Eq. (9) is evaluated for the full angular range. The average value of $W_{AT}(E, h)$ was then determined for the given equatorial altitude. The average fraction of remaining neutral hydrogen was also calculated as a function of energy, and $W_{AT}(E, h)$ as a function of both energy and altitude as shown in Fig. 5. The figure shows 4 curves at specified energy values and then weighted average over the whole energy range based on an $E^{-2.55}$ energy spectrum. The remaining proton fraction is normalized to 0.5 at 600 km. A strong altitude gradient of the fraction of undepleted neutrals starting from approximately 400 km is indicated.

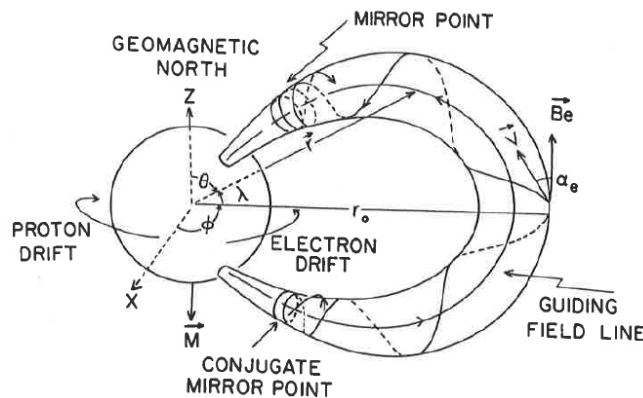


Fig4. Trapping mechanism of charged particles by performing cyclotron motion around magnetic field lines, bouncing back and forth between two mirror points, and drifting around the Earth.

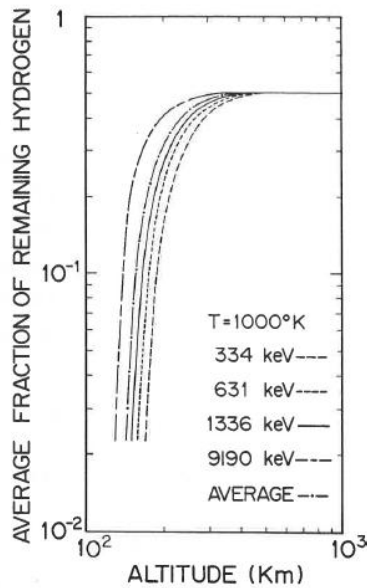


Fig5. Altitude vs average fraction of remaining neutrals at different energies

The undepleted neutrals will be converted to protons according to this relation

$$j_p(E, h) = [\sum_{01}(h,E)/\sum_{10}(h,E)]j_{H}(h,E) \quad (10)$$

The surviving protons at any altitude as detected in the Phoenix-1 experiment, are then given by the product of the survival probability for ionization loss ($1-W_{10}$) which depends on the instrumental threshold, the sampling efficiency of the instrument in pitch angle space combined with the pitch angle distribution function, which is called loss cone effect W_{LC} , and $j_p(E, h)$.

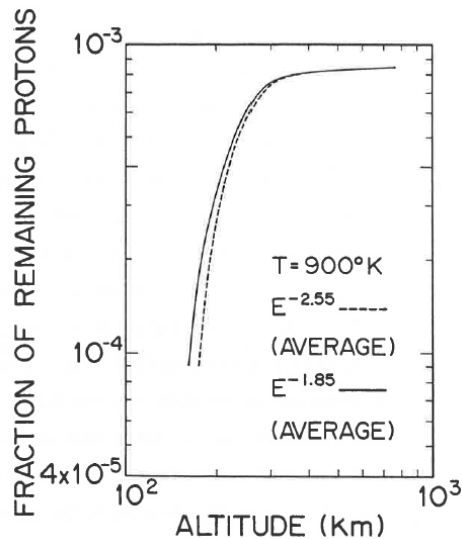


Fig6. Surviving protons vs. altitudes at two different spectral indices showing that the effect of altitude dependence is not significant if the spectral index is reduced from 2.55 to 1.85

2.3. Proton survival from Ionization loss

Ionization loss of protons occur through Coulomb excitation energy loss in the atmosphere. A quasi-trapped proton at any equatorial altitude loses some energy ΔE in its lifetime in bouncing between two mirror points (Fig. 4).

The spiral arc length traversed by a proton of equatorial distance r_o is given by Eqs.

$$s(\alpha_e) \sim 1.38 - 0.32(\sin\alpha_e + \sqrt{\sin\alpha_e}) \quad (11)$$

and

$$dl^* = dl/\cos\alpha = r_o s(\alpha_e) \quad (12)$$

Within $0 \leq \alpha_e \leq \pi/2$, the bounce period varies less than a factor of 2. The spiral length dl^* and the field arc length dl and the local pitch angle α are related by Eqn. (12) which shows almost independence of dl^* upon pitch angle.

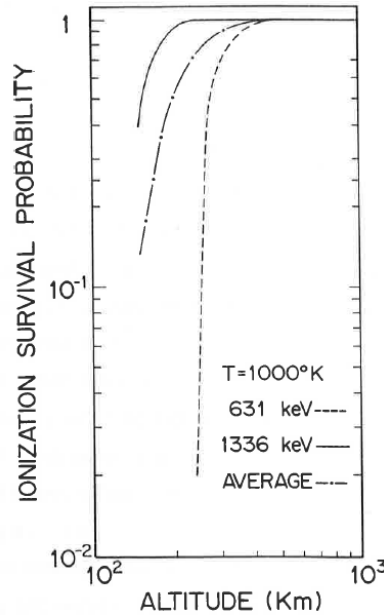


Fig7. Ionization survival probability vs altitude at 631 keV, 1336 keV, and the average probability for the entire energy range

Multiplying the bounce average density corresponding to the given α_e and r_o , by the spiral arc length, we get the atmospheric column density experience by the proton. Energy loss of protons was calculated in a diatomic oxygen atmosphere, and, if the proton energy fell below 0.60 MeV, it was not detected. The ionization loss probability is defined as

$$W_{IO}(E, h) = \Delta E / (E - E_{thrs}) \quad (13)$$

where E_{thrs} is the threshold = 600 keV. For a single particle, if $E > E_{thrs}$, the particle will be detected. However, its detectability depends also upon the energy ΔE it loses. If ΔE is zero, the surviving probability is 1. On the other hand, if ΔE is such that the energy has been reduced to E_{thrs} , the surviving probability vanishes. And ΔE depends upon the proton pitch angle, proton energy, and the altitude. The characteristics of $W_{IO}(E, h)$ has to be the following:

- The higher the altitude, the lower the value of $W_{IO}(E, h)$,
- The higher the energy, the lower the $W_{IO}(E, h)$, and
- The higher the difference $|90^\circ - \alpha_e|$, the higher the $W_{IO}(E, h)$

The energy loss bears the signatures of these three effects. In a distribution of particles, $W_{IO}(E, h)$ represents the loss probability of particles of energy greater than 600 keV. The corresponding ionization survival probability function is defined as

$$1 - W_{IO}(E, h) = 1 - \frac{\Delta E}{E - E_{thrs}} \quad (14)$$

Table II shows ΔE as a function of E and α_e . Fig. 7 shows the ionization survival probability at 631 keV, 1336 keV, and the average probability for the entire energy range. The probability function is normalized to unity at 600 km.

Below 150 km, the probability function value is not shown. In the calculation, ΔE represents the energy loss in a bounce path. Steep curves appear at low altitudes and energies.

Table2. Ionization Survival Probability

h	E	α_e	τ_{CE}	# of	Drift	ΔE
(km)	(keV)	(deg)	(sec)	Bounces	Period (min)	(keV/Bounce)
200	631	90	0.764	0.431	40.59	104
		85.7	0.694	0.391	40.62	115
	1336	90	6.730	5.530	13.23	61.2
		85.7	6.120	5.020	13.24	67.5
250	631	90	2.810	1.580	40.28	28.2
		85.7	2.550	1.410	40.31	31.2
	1336	90	24.80	20.20	13.13	16.6
		85.7	22.40	18.30	13.14	18.4
300	631	90	8.350	4.650	39.98	9.50
		85.7	7.860	4.360	40.14	10.1
	133	90	73.70	59.60	13.03	5.60
		85.7	69.30	56.00	13.04	5.96

2.4. Loss Cone Effect

So far we are dealing with $\alpha_e=90^\circ$ particles at the equator, but we can extend the treatment to include particles of all other pitch angles. We can think of neutrals reaching other latitudes, and can similarly, as mentioned in the paragraph of Eq. (9), find their contribution at those latitudes. However, an easier way to include them is through a weighting factor W_{LC} which takes care of the increased equatorial pitch angle ranges with increasing altitude and the instrument's efficiency to detect particles of different equatorial pitch angles. Table I shows the equatorial pitch angle ranges in different equatorial altitude ranges. With decreasing altitude, the magnetic field has decreasing capability of keeping particles trapped/quasi-trapped, since the size of the loss cone is a function of the equatorial altitude (Eq. (3)). W_{LC} is equal to the right hand side of Eq. (15.) (which is an integral of the product function of equatorial pitch angle distribution and the instrumental efficiency), with the appropriate limits of integration taken as a function of altitude, i.e.

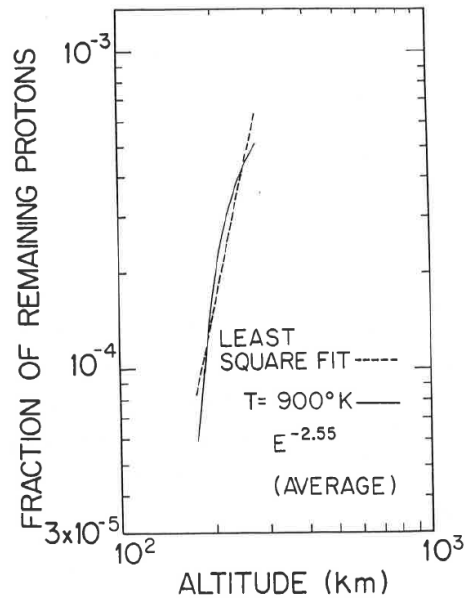
$$W_{LC} = \sum F(\alpha_j) f(\alpha_j) d\alpha \quad (15)$$

where $F(\alpha_j) = \sin^{13} \alpha_j$ has been used as the pitch angle distribution function. The values of W_{LC} are listed in Table III for the pitch angle ranges relevant to different altitudes

Table III W_{LC} for Different Altitudes and Pitch Angle Ranges

Altitude (km)	Pitch angle Range (deg)	W_{LC} (Normalized at 800 km)
175	90±12	0.645
200	90±14	0.808
250	90±17	0.889
300	90±20	0.924
350	90±22	0.964
400	90±24	0.979
450	90±26	0.989
500	90±28	0.994
600	90±31	0.998
800	90±36	1.000

W_{LC} is not a strong function of altitude. In the observational altitude range it varies by a factor or ~ 1.4 . At any altitude it depends on the pitch angle distribution and the instrumental efficiency. It does not depend on energy since we assume $f(\alpha)$ in Eqn. (15) is independent of energy.



III. RESULT AND DISCUSSION

The final fraction of protons of energy E surviving at altitude h is given by

$$f_p(E, h) = W_{LC} (1 - W_{IO}) W_{AT} \quad (16)$$

We have done a least square fit to this function in the altitude range 175 to 275 km. To get this function at any altitude, we multiplied the average of both $(1 - W_{IO})$ and W_{AT} over the entire energy range of the instrument, weighted by $E^{-2.55}$ spectra. The product function has been plotted in Fig. 8 as a function of altitude. To find the power law represented by the solid line within the observational altitude range for comparison with fifth power altitude dependence of flux, a least square fit was done. The dotted line represents the least square fit line. It has a slope of 4.56 ± 0.26 . This explains closely the observed 5th power altitude dependence of the measured proton flux in our observational altitude range. To evaluate $f_p(E, h)$ we have used Jacchia atmosphere (1977) at 900° K which was the mean temperature for the local time of the Phoenix – 1 observations.

Since we did not consider any secondary generation of protons in the model, the agreement between the observed and the model predicted slopes indicates that the primary proton flux will outnumber the secondary or higher order generation of proton flux, or in other words, secondary or higher order generation of protons will not have a significant effect upon the protons produced from the primary beam of incident neutrals.

The turnover of the altitude variation curve beyond 300 km also explains the altitude independence of the proton flux reported by Moritz (1972).

IV. CONCLUSION

The charge exchange loss coupled with the loss cone effect can explain the fifth-power altitude variation of magnetospheric particle precipitation at low altitude near the geomagnetic equator.

REFERENCES

- [1] Adel, M.M., 2008. A detector telescope's pitch angle sampling of magnetospheric particles. *Earth, Planets Space*, 60: 753-761.
- [2] Adel, M. M., 2012. Absolute flux comparison of magnetospheric particles, *Physics International.*, 3:1-8; DOI: 10.3844/pisp.2012.1.8; URL: <http://thescipub.com/abstract/10.3844/pisp.2012.1.8>
- [3] Adel, M. M., 2013. Rotation matrix method for calculation of a detector telescope's response function, *Projournal of Physical Science Research*, Vol. 1(2), pp.14-30, September 2013; nline: <http://www.projournals.org/PPSR>

- [4] Cabera, J., M. Cyamukungu, P. Stauning, A. Leonov and P. Leleux et al., 2005. Fluxes of energetic protons and electrons measured on board the Oersted satellite. *Ann. Geophys.*, 23: 2975-2982.
- [5] Guzik, T.G, M. A. Miah, J. W. Mitchell, and J. P. Wefel, 1987. Low energy protons at the equatorial zone, *Journal of Geophysical Research*, vol. 94, pp. 14-21
- [6] Hovestadt, D., B. Hausler and M. Scholer, 1972. Observation of energetic particles at very low altitudes near the geomagnetic equator. *Phys. Rev. Lett.*, 28: 1340-1344.
- [7] Miah, M.A., 1988. Global Zones of Particle Precipitation. Ph. D. Thesis, Department of Physics and Astronomy, Louisiana State University, Baton Rouge.
- [8] Miah, M. A., 1989. Observation of low energy particle precipitation at low altitude in the equatorial zone, *Journal of Atmospheric and Terrestrial Physics*, vol.51, pp.541-550
- [9] Miah, M. A., 1990. Observation of $Z \geq 1$ particles below 300 km near the geomagnetic equator, *Journal of Geomagnetism and Geoelectricity*, vol. 43, pp. 461-472.
- [10] Miah, M. A., 1991. Global proton peak flux profile in the equatorial zone, *Indian Journal of Radio and Space Science*, vol. 20, pp.12-24
- [11] Miah, M. A., 1991. ONR-602 experiment to investigate particle precipitation near the equator, *Journal of Geomagnetism and Geoelectricity*, vol. 43, pp.445-454.
- [12] Miah, M. A., J. W. Mitchell, and J. P. Wefel, 1989. Magnetospheric particle detection efficiency of a conical telescope, *Nuclear Instrumentation and Methods in Physics Research*, vol. A281, pp. 622-632
- [13] Miah, M. A., 1993. Solar-induced variation of proton precipitation near the equator, *Journal of Atmospheric and Terrestrial Physics*, vol.55, no. 9, pp.1295-1301
- [14] Miah, M. A., 1993. Solar cycle dependence of equatorial protons in the thermosphere, vol. 2, p. 721, in Hruska,
- [15] Shea, Smart, and Heckman, eds., *Proceedings of the Solar-Terrestrial Predictions - IV Workshop*, Montreal, Canada
- [16] Miah, M. A., 1994. Phoenix-1 observation of storm-time precipitation of ring current particles, *UAPB Research Journal*, vol.1, pp.45-54
- [17] Miah, M. A., 1994. Significant variation of proton precipitation in equatorial thermosphere, *Advances in Space research*, vol.14, no. 9, pp.229-235
- [18] Miah, M. A., 1994. EXOS-C project at UAPB, *UAPB Research Journal*, vol. 1, pp.17-25
- [19] Miah, M.A., J.W. Mitchell and J.P. Wefel, 1989. Magnetospheric particle detection efficiency of a conical telescope. *Nucl. Instr. Meth. Phys. Res.*, 281: 622-627. DOI: 10.1016/0168-9002(89)91499- X *Phy. Intl.* 3 (1): 1-8, 2012 8
- [20] Miah, M.A., K. Nagata, T. Kohno, H. Murakami and A. Nakamoto et al., 1992. Spatial and temporal features of 0.64-35 MeV protons in the space station environment: EXOS-C observations, *J. Geomagnetism Geoelec.*, 44: 591-610.
- [21] Miah, M. A., K. Nagata, T. Kohno, H. Murakami, A. Nakamoto, N. Hasebe, J. Kikuchi, and T. Doke, 1992. Spatial and temporal features of 0.64-35 MeV protons in the Space Station environment: EXOS-C observations, *Journal of Geomagnetism and Geoelectricity*, vol. 44, pp. 9-20.
- [22] Mizera, P.F. and J.B. Blake, 1973. Observations of ring current protons at low altitudes. *J. Geophys. Res.*, 78: 1058-1062. DOI: 10.1029/JA078i007p01058
- [23] Moritz, J., 1972. Energetic protons at low equatorial altitudes. *Zeitschrift fur Geophysik*, Band, 38: 701-717.
- [24] Scholer, M., D. Hovestadt and G. Morfil, 1975. Energetic He⁺ ions from the radiation belt at low altitudes near the geomagnetic equator. *J. Geophys. Res.*, 80: 80-85. DOI: 10.1029/JA080i001p00080
- [25] Sullivan, J.D., 1971. Geometrical factor and directional response of single and multi-element particle telescopes. *Nucl. Instruments Meth.*, 95: 5-11. DOI: 10.1016/0029-554X(71)90033-4
- [26] Toburen, L. H., M. Y. Nakai, and R. A. Langley, 1968. Measurements of high energy charge-transfer cross-sections for incident protons and atomic hydrogen in various gases, *Physical Review*, Vol. 171, No. 114.

- [27] Yusif, A.K., I.B. Bahari and M.S. Yasin, 2010. Identifications of the specific relations among physical parameters which use to quantify interaction effect of charged particles at low dose. *Phys. Int.*, 1: 90-94. DOI: 10.3844/pisp.2010.94.98
- [28] Wentworth, R. C., 1960. Lifetimes of geomagnetically trapped particles determined by Coulomb scattering, Ph. D. Thesis, University of Maryland, p.112.